Mon. Not. R. Astron. Soc. **000**, 000–000 (0000) Printed 13 October 2011 (MN LATEX style file v2.2)

Exploring the links between star formation and minor companions around isolated galaxies

Jacob P. Edman, Elizabeth J. Barton, and James S. Bullock[1]
[1] *Center for Cosmology, Department of Physics and Astronomy, University of California, Irvine, CA 92697-4575 (email: ebarton@uci.edu)*

9 October 2011

ABSTRACT

Previous studies have shown that galaxies with minor companions exhibit an elevated star formation rate. We reverse this inquiry, constructing a volume-limited sample of $\sim$L* ($M_r \leq -19.5 + 5\log h$) galaxies from the Sloan Digital Sky Survey that are isolated with respect to other luminous galaxies. Cosmological simulations suggest that 99.8% of these galaxies are alone in their dark matter haloes with respect to other luminous galaxies. We search the area around these galaxies for photometric companions. Matching strongly star forming (EW(Hα)$\geq$ 35 Å) and quiescent (EW(Hα)$<$ 35 Å) samples for stellar mass and redshift using a Monte Carlo resampling technique, we demonstrate that rapidly star-forming galaxies are more likely to have photometric companions than other galaxies. The effect is relatively small; about 11 % of quiescent, isolated galaxies have minor photometric companions at radii $\leq$ 60 kpc h^{-1} kpc while about 16 % of strongly star-forming ones do. Though small, the cumulative difference in satellite counts between strongly star-forming and quiescent galaxies is highly statistically significant ($P_{KS} = 1.350 \times 10^{-3}$) out to to radii of $\sim$ 100 h^{-1} kpc. We discuss explanations for this excess, including the possibility that $\sim$ 5% of strongly star-forming galaxies have star formation that is causally related to the presence of a minor companion.

Key words: galaxies: formation, halos, interactions, evolution, statistics

1 INTRODUCTION

Many studies have established that the environmental properties of galaxies are closely related to their star formation histories (e.g., Dressler 1980; Postman & Geller 1984). On large scales, stronger clustering effects are observed in red galaxies than in blue galaxies, because red galaxies also tend to be more massive and reside in more massive dark matter halos (see Zehavi et al. 2011, and references therein). However, at scales less than $\sim$ 300 kpc, where galaxies are likely to be part of the same halo, these clustering effects are poorly understood, and at scales less than 50 kpc, blue galaxies may cluster more strongly (Masjedi et al. 2008).

Previous studies establish that galaxy interactions and the presence of a companion are both associated with an increased rate of star formation (Barton et al. 2000; Lambas et al. 2003; Larson & Tinsley 1978; Mihos & Hernquist 1994, e.g.). In particular, closer companions lead to increased rate of star formation for both major and minor interactions (Barton et al. 2000; Lambas et al. 2003; Nikolic et al. 2004; Woods et al. 2006, e.g.). These results are qualitatively in line with expectations from numerical simulations that predict enhanced star formation in interacting pairs before the galaxies finally merge (Barnes & Hernquist 1996; Mihos & Hernquist 1994, e.g.). though those results are sensitive to uncertain star formation physics (e.g. (Cox et al. 2006)). In principle, close passes in both major and minor pairs can initiate a burst of star formation.

The questions that surround minor mergers are closely related to the properties of the satellite galaxies and their hosts. The radial distribution of satellites around primary galaxies has been extensively explored. Chen (2008) finds that the radial distribution of blue satellites around isolated hosts is significantly shallower than that of red satellites. There were also hints in this study that red and blue hosts may have different satellite distributions (Chen 2008). Previous studies have also examined the effects of galaxy color on the anistropic distribution of satellite galaxies around their hosts (Agustsson & Brainerd 2007; Azzaro et al. 2007; Bailin et al. 2008; Kang et al. 2007). For red central galaxies, satellites tend to be more strongly aligned along the major axis, while the distribution of satellites for blue central galaxies are consistent with an isotropic distribution. These observations further demonstrate the expectation that rela-

tionships exist between galaxy color and satellite distribution.

Some studies reveal a deficiency of satellites at very small radii (less than 20 kpc) compared to the extrapolated outer density profile (Sales & Lambas 2005; van den Bosch et al. 2005). This deficiency may be due to a failure to resolve interacting pairs into single galaxies, or it could be a real deficiency due to galaxy destruction. Sales & Lambas (2005) find that this deficiency can be predictably be found in poorly star forming galaxies, which tend to have larger core radii, while strongly star forming galaxies often have more close neighbors than predicted (Sales & Lambas 2005). This finding lends support to the long-established hypothesis that interaction with a nearby galaxy often causes enhanced star formation.

Despite our knowledge that both major and minor interactions trigger star formation, the complete cosmological impact of these processes remain unknown. When galaxies do exhibit significantly enhanced star formation, it is not known how often that star formation is related to an interaction. Here, we invert the standard approach to minor mergers by identifing a volume-limited sample of $\sim$L* galaxies that are isolated with respect to other luminous galaxies in from the Sloan Digital Sky Survey Data Release 6 (SDSS6 Adelman-McCarthy et al. 2008). We then compare the photometric companion counts around the star-forming galaxies to the counts around other galaxies. In § 2, we describe the initial galaxy sample and search procedures. § 3 describes the bias corrections we apply to ensure a fair comparison. We describe the results in § 4, discuss them in § 5, and conclude in § 6.

2 SAMPLE

We begin by identifying a set of galaxies in the Value Added Galaxy Catalog of SDSS DR6 (Adelman-McCarthy et al. 2008, VACG),(Blanton et al. 2005). We restrict the sample to sources that are isolated with respect to other luminous galaxies. We compile all sources in the Sloan Digital Sky Survey Data Release 6 that are more luminous than $M_r + 5$ log (h)= -19.5 at a redshift $z < 0.0804$, which is the upper limit at which a galaxy of this luminosity will appear in the spectroscopic sample. We then identify galaxies that have no neighbors within a projected distance of 400 kpc h^{-1} and 1000 km s^{-1}of the primary, and at most one neighbor within 700 kpc h^{-1} and 1000 km s^{-1}. These conservative isolation criteria include neighbors with measured redshifts and potential neighbors which are in the photometric survey but do not have measured redshifts. For example, a galaxy with a potential luminous neighbor with unmeasured redshift at 300 kpc h^{-1} will be rejected.

These criteria result in a sample of 24,753 isolated central galaxies. Using the techniques of Barton et al. (2007), we employ cosmological simulations to demonstrate the expected purity of this sample. The method relies on assuming that halo circular velocities in simulations scale monotonically with M_R. The space density of galaxies with $M_r + 5log(h) = -19.5$ in SDSS, computed by integrating the luminosity function of (Blanton et al. 2003), corresponds to halos that had circular velocities $\geq$ 164 km s^{-1}at the present epoch, or at the time they became substructure if they are not central sources in the hybrid n-body and semi-analytic simulations of (Zentner et al. 2005). Forming an artificial redshift survey with these galaxies and applying selection criteria that are identical to those applied to the data, we show that 99.8% of the isolated sample consists selected via our isolation criteria galaxies that are alone in their dark matter halos (with respect to other galaxies with $M_r \leq -19.5 + 5\log(h)$).

Table 1. Sample sizes for complete and corrected samples

cutoff type	cutoff	star-forming	quiescent
g-r	0.4	1825	22435
EW(Hα)	35Å	1951	16467
g-r (Corrected)	0.4	1388	7180
EW(Hα)(Corrected)	35Å	1566	7180

A subset of the SDSS central galaxies are near the edges of the survey, in less complete regions, or close to bright stars. As a result, we may not be completely probing their environments for potential companions. We thus identify a "complete environment" subsample of galaxies using the tools available in the VACG. In particular, we remove the lowest and highest redshift sources so that we can probe the entire 1000 km s^{-1}in front of and behind the galaxies. Then, we use the random subsamples provided in the VACG, weighted by completeness of each sector and weighted based on the magnitude limit of the survey in that sector. We add the "random counts" in each galaxy's relevant environment, in essence performing a Monte Carlo integration of its environment weighted by completeness. We then restrict the "complete environment" subsample to the 18,601 galaxies where the value of this integral is within 2σ of the mode for the entire distribution. We explore whether restricting to this subsample affects any of our results. Because it does not have any qualitative effect, we confine our discussion to the original 24,853 isolated galaxy sample hereafter.

We use the SDSS Data Release 7 online database to tabulate potential minor companions to an angular radius that would correspond to 200 h^{-1} kpc from each central galaxy, with an apparent magnitude limit of $m_R = 21$. In the remaining sections of the paper, we explore the dependence of the companion counts on galaxy properties.

3 BIAS CORRECTIONS

In this study, we focus on the counts of potential faint companion galaxies around otherwise isolated $\sim$L* central galaxies. In particular, we separate pair samples into rapidly star-forming galaxies and galaxies that are not rapidly star forming. Because we do not have redshifts for these potential comanions, we must count them in an angular radius around the centrals. In addition, because we count them to a fixed flux limit, the study will include relatively less luminous companions around nearby galaxies. As a result, any differences in the redshift distributions of two samples of galaxies that we compare will cause potential biases in the comparisons. Because galaxies are known to cluster, and because satellites should be more numberous around more massive galaxies, halo mass is another key parameter that must be controlled when comparing two samples. No direct

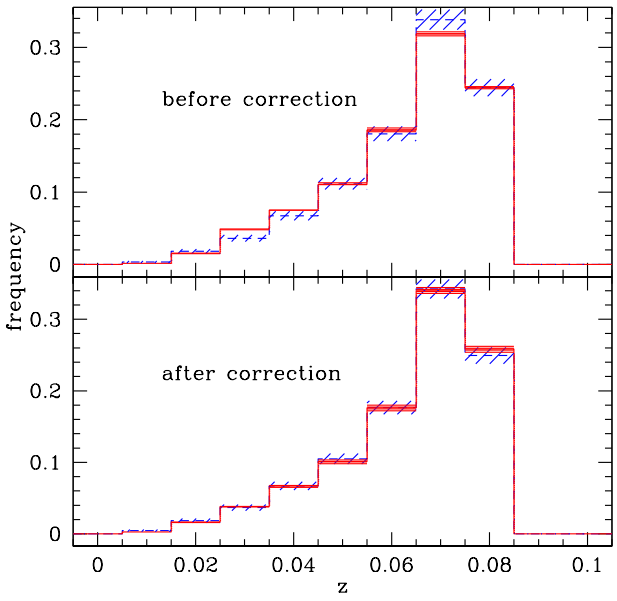

Figure 1. *Top:* The redshift distribution of central galaxies for the complete sample of galaxies. *Bottom:* The redshift distribution of central galaxies is shown for a corrected sample. For both plots, the blue dashed line depicts galaxies with EW(Hα)$\geq$ 39 Å and the red solid line shows galaxies with EW(Hα)¡ 35 Å. Error bars are calculated for each bin as $\sqrt{n}/n_{total}$.

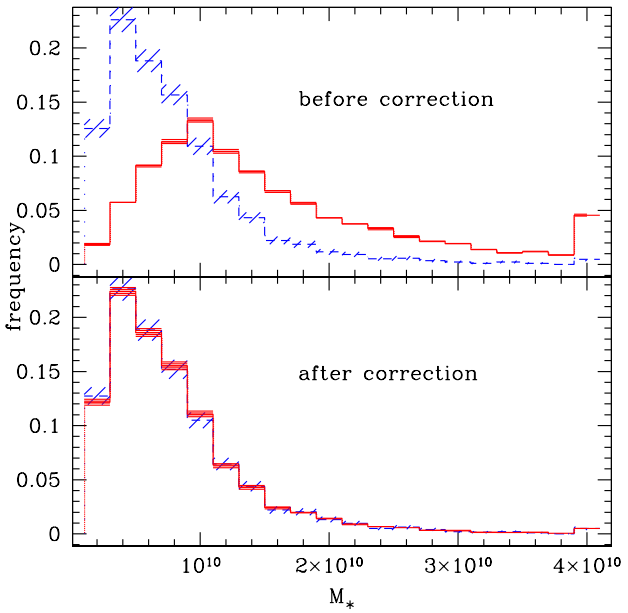

Figure 2. *Top:* The stellar mass distribution of central galaxies for the complete sample of galaxies. *Bottom:* The stellar mass distribution of central galaxies is shown for a corrected sample. For both plots, the blue dashed line depicts galaxies with EW(Hα)$\geq$ 35 Å and the red solid line shows galaxies with EW(Hα)¡ 35 Å. Error bars calculated for each bin as $\sqrt{n}/n_{total}$.

measure of halo mass is available, so we use stellar mass as a proxy. In this section, we describe our simple techniques to resample the data in order to compare galaxies with the same distributions of redshift and stellar mass.

We employ a Monte-Carlo random selection method to compare the radial distributions of neighbors around blue and red central galaxies with similar redshifts and stellar masses. Our Monte-Carlo simulation selects a random sample of 5 red galaxies with similar redshift and stellar mass to each of the blue galaxies in the sample. A red galaxy is considered similar to the blue galaxy if z is within ± 0.005 and the stellar mass is within ± 10%.

Figure 1 depicts the redshift distributions of strongly star-forming and quiescent central galaxies, based on EW(Hα) cutoff of 35 Å, for the complete sample and one of the subsamples derived using our Monte-Carlo selection method. Visually, the redshift distributions of the strongly star-forming and quiescent galaxies in the complete sample are significantly different. There is an excess of strongly star-forming galaxies at lower redshifts when compared to the quiescent galaxies. The corrected sample appears to match much more closely. This interpretation is supported by the Kolmogorov-Smirnov test results, which are reported in Table 2. P_{KS} (z) = 5.417×10^{-9} for the full sample, which indicates that the redshifts of star-forming and quiescent galaxies have a different distribution. For the corrected sample, P_{KS} (z) = 0.5746, so the two subsamples likely are drawn from the same distribution.

The stellar mass distributions for the complete sample, plotted in the top of Figure 2, are even more disparate than the redshift distributions. As expected, there is an excess of centrals with EW(Hα)$<$ 35 Å in the high-mass range, and

Table 2. Results of Kolmogorov-Smirnov test for redshift and stellar mass distributions of EW(Hα)separated central galaxies and Monte-Carlo samples

Sample type	cutoff	P_{KS} (z)	P_{KS} (stellar mass)
Complete	EW(Hα)= 35 Å	0.01688	0
Complete	g-r = 0.4	5.417×10^{-9}	0
Corrected	EW(Hα)= 35 Å	0.249 - 0.696	0.818 - 0.969

an excess of centrals with EW(Hα)$>$ 35 Å in the low mass range. The extremely low P_{KS} (z) and P_{KS} (stellar mass) values for the subsamples taken from the complete set of central galaxies demonstrate that they have extremely different redshift and stellar mass distributions. The Monte-Carlo derived sample, plotted at the bottom of Figure 2, provides a much better visual match between the stellar mass distributions of strongly and not strongly star-forming central galaxies. Once again, this interpretation is supported by the KS test results, which are shown in Table 2. We show the KS statistics from 10 Monte-Carlo simulations, and KS (z) ranges from 0.249 - 0.696 and the KS (stellar mass) spans 0.818-0.969.

Additionally, because we necessarily observe a two-dimensional view of astronomical objects, our sample of potential satellites is contaminated by interlopers, i.e. objects that are not physically within our searched radius but nevertheless appear to be true companions when projected on the sky. Overall, interlopers tend to flatten the projected radial mass distribution, and the fraction of observed satellites that are actually interlopers increases with search radius. (Chen et al. 2006) tested both volume limited and flux lim-

ited samples (which are biased towards brighter satellites) and found consistent radial distributions, showing that there is at best a limited dependence of interloper contamination on magnitude of the satellites and color of the primaries. Sales and Lambas (2005) find a flat distribution of interlopers between 20 and 500 kpc by specifically sampling for companion galaxies with a large projected velocity difference ($2000 < |\Delta V| < 10000$ km s^{-1}) compared to the central, allowing them to assume a uniform contamination when calculating the radial density profiles of satellites.

For our study, interloper contamination will obscure the relationship between close satellites and blue hosts, because red galaxies tend to be more massive and reside in larger dark matter halos than blue galaxies. This larger halo size means there is a stronger clustering effect on scales of ~ 300 kpc and larger (Masjedi et al. 2008). When searching on small radial scales (for example, less than 100 kpc) there should be minimal contamination, but potential satellites at larger radii in these larger dark matter halos are more likely to be interlopers because the environment is more crowded. Assuming a isotropic background, if interlopers are a significant factor in our study, we would expect the radial distribution of satellites to be roughly proportional to r^2. However, as we shall demonstrate below, the radial distribution we observe scales closer to $\sim$r. At small radii, the true companions appear to dominate.

4 RESULTS

We compare the list of potential companions with their associated central galaxies and compute the projected radial distance to each companion, throwing out any companions at a distance that exceeds the specified search radius, or that have a Petrosian r magnitude greater than 21. For our primary analysis, we choose to set the red-blue cutoff for our central galaxies at EW(Hα)= 35 Å. This cutoff allows us to examine only the most strongly star forming galaxies, giving us the best chance of detecting the effect of close neighbors on galaxy star formation activity.

4.1 Numbers of neighbors

In figures 3(a) and 3(b), we demonstrate that strongly star-forming central galaxies are more likely to have a close neighbor. Figure 3(a) contains histograms of the frequency of a central galaxy having a given number of neighbors within 100 kpc for the complete (top) and corrected (bottom) samples. We choose to plot 100 kpc because closer neighbors are associated with more recent starbursts, and thus larger stellar populations in the blue spectral range (Barton et al. 2000). Again, the central galaxies are grouped into strongly star-forming and quiescent subsamples, with the cutoff at EW(Hα)=35 Å. The quiescent central galaxies are represented by the solid red line and the strongly star-forming centrals by the dashed blue line. The frequency is expressed as a fraction of the total neighbors in each category.

For both the complete and the corrected sample, there is an excess of strongly star-forming central galaxies with one or two neighbors within 100 kpc. We find that the KS probability that the neighbor distributions are the same is zero, indicating an extremely high degree of significance. For

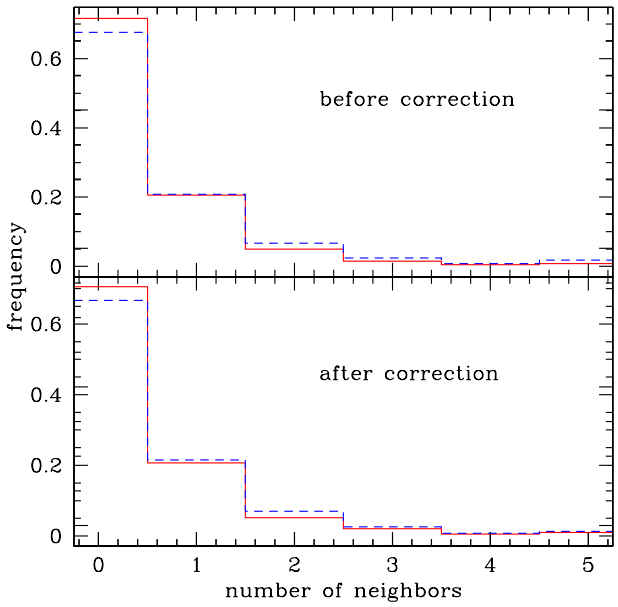

(a)

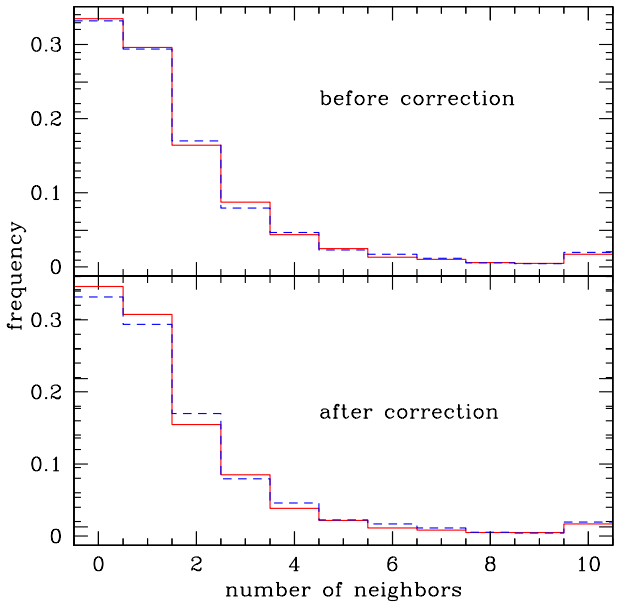

(b)

Figure 3. Histograms of the number of neighbors for each central galaxy within 100 kpc (top) and 200 kpc (bottom). Within each plot, the top plot is the complete sample and the bottom is the corrected sample. The blue dashed line indicates central galaxies with EW(Hα)$\geq$ 35 Å; the red solid line indicates central galaxies with EW(Hα)¡ 35 Å.

greater numbers of neighbors, the red and blue lines are nearly identical. Figure 3(b) is similar to the figure 3(a) but for a radius of 200 kpc. At this radius, the distribution of number of neighbors for both types of centrals centrals is more similar, but $P_{KS} = 0$, which indicates again that the observed (small) difference has a high degree of significance.

We made similar plots for radii ranging from 20 to 200

kpc, and a few trends become obvious. As the search radius decreases, the difference between star-forming and quiescent centrals becomes magnified, indicating that there is a relationship between star formation and distance to the nearest companion (Chen et al. 2006). With increasing radius, the line representing the quiescent central galaxies becomes closer and closer to the blue line, until they become nearly indistinguishable around 150 kpc. This behavior is expected, because at large radii, the effect a companion can have on triggering star formation is small. Additionally, the signal is increasingly dominated by interlopers as the searched radius increases. Finally, star-forming galaxies tend to have one close neighbor, while quiescent galaxies tend to have a large number of neighbors at larger distances away. This result indicates that some of the star-forming central galaxies may be part of an interacting pair of galaxies, possibly triggering a burst of star formation.

The behavior of the quiescent centrals arises because red galaxies are more massive and thus can be expected to cluster more strongly. For all samples at all radii, Kolmogorov-Smirnov tests indicate a very high degree of statistical significance ($> 99.999\%$) for the difference between distributions of number of neighbors, whether divided by g-r color or EW(Hα). Ultimately, these plots suggest that star-forming central galaxies tend to have more near neighbors than quiescent central galaxies, which lends support for the idea that many are because of a triggered star formation event.

4.2 Radial distribution of neighbors

After showing that central galaxies above the EW(Hα) cutoff are somewhat more likely to have a near neighbor than centrals below the cutoff, we quantify difference in radial distribution of satellites between the strongly star-forming and less star-forming centrals. For this, we use the redshift and stellar mass corrected Monte-Carlo samples. Each Monte-Carlo sample chooses 5 red central galaxies similar to each blue central. In figure 4, we plot the radial distribution of neighbors for 10 of these Monte-Carlo samples in two different ways.

Figure 4(a) shows the fraction of central galaxies with at least one neighbor in each annulus, with annulus bins in steps of 10 kpc. The blue dashed line represents centrals with EW(Hα)$>$ Å and the red lines are the quiescent centrals with EW(Hα)$\leq$ 35Å. There is some variation of the quiescent subsamples because of the random selection, but it is well within the Poisson error bars shown. Inside 85 kpc, central galaxies above the EW(Hα)break are significantly more likely to have a neighbor. This result clearly indicates that the strongly star-forming galaxies are more likely to have a neighbor nearby. Beyond 85 kpc, the plot gets noiser, and there is little significant difference between the red and blue lines. We expect this because at such large radii a neighboring galaxy can have little direct effect on the star formation of the central galaxy, and interlopers begin to dominate (Tollerud et al. 2011).

Figure 4(b) is similar to figure 4(a), but instead we plot the cumulative fraction of central galaxies with at least one neighbor inside a given radius. At the innermost bin, centered at 5 kpc, the gap narrows; objects separated by less than 3 kpc (including mergers, which are often associated with bursts of star formation) are nearly impossible for the detector to resolve. We find that the cumulative difference between star-forming and quiescent centrals is significant out to 100 kpc, implying that star-forming galaxies are $\sim 5\%$ more likely to have at least one neighbor within 100 kpc than quescent galaxies of the same stellar mass. However, the overall fraction of star-forming galaxies with a neighbor within 100 kpc is still small.

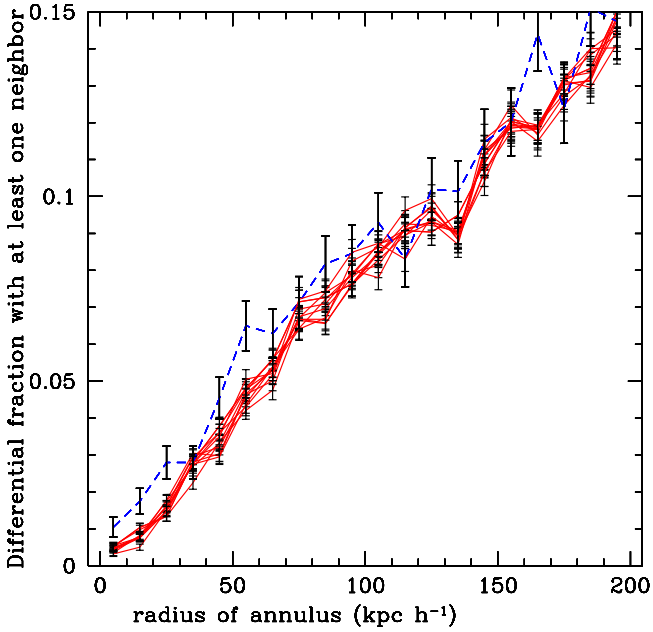

(a)

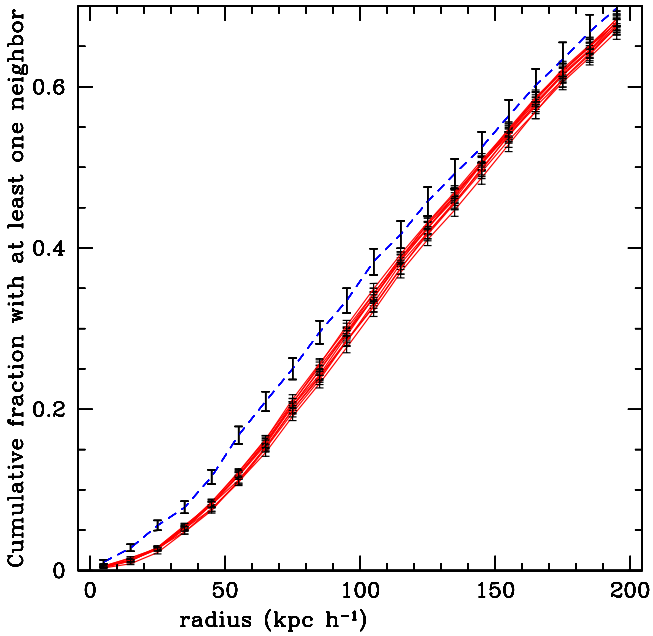

(b)

Figure 4. *Top*: The fraction of central galaxies with at least one neighbor in decadal bins ranging from 0 - 200 kpc for 10 Monte-Carlo selected samples. The blue dashed line indicates strongly star-forming galaxies with EW(Hα)$\geq$ 35 Å, while the red solid lines are centrals with EW(Hα)$<$ 35 Å. :Bottom: Similar to *Top*, but here we plot the cumulative fraction of centrals with at least one neighbor within a given radius for 10 Monte-Carlo samples.

Table 3. Results of Kolmogorov-Smirnov test for nearest neighbor distributions of central galaxies

Sample type	comparison cutoff	P_{KS} (neighbor)
Complete	EW(Hα)= 35 Å	0.02642
Complete	g-r = 0.4	.01445
Corrected	EW(Hα)= 20 Å	8.452×10^{-2}
Corrected	EW(Hα)= 35 Å	1.350×10^{-3}
Corrected	EW(Hα)= 40 Å	8.615×10^{-3}
Corrected	g-r = 0.4	0.1390
Corrected	g-r = 0.5	0.1022
Corrected	g-r = 0.6	2.269×10^{-3}

The difference in nearest neighbor distribution between strongly star-forming and quiescent galaxies is significant as demonstrated by the KS statistics, which are tabulated in Table 3. Here we present comparisons for several choices for how to divide the populations between quiescent or red galaxies and star-forming or blue galaxies, as specified by a "cutoff" criterion in the middle column, either in g-r color or EW(Hα). The Corrected samples used in this analysis contain 20 quiescent or red central galaxies for each strongly star-forming or blue central galaxy.

The Complete sample statistics, presented in the top two rows, include the entire sample of 24,753 galaxies, uncorrected for redshift or stellar mass. We find the neighbor distributions within the Complete sample to be marginally different for cutoffs at both g-r = 0.4 and EW(Hα)= 35 Å, with P_{KS} values of 0.01445 and 0.02646, respectively. The Corrected samples demonstrate more significant differences. The highest degree of significance is found for the cutoff at EW(Hα)= 35 Å, which has $P_{KS} = 1.350 \times 10^{-3}$. However, when our resampling method is applied using g-r color as the cutoff, the difference between the nearest neighbor distributions for blue and red central galaxies becomes less significant, possibly due to the differing timescales of g-r as an indicator of recent star formation or simply a consequence of the reduced sample size. Using g-r color as a proxy for star formation is also prone to errors due to dust-reddening, which would tend to cancel out the effect we see when using EW(Hα).

Figure 5 is a histogram of the differences in apparent r-band magnitude for each companion and its host. The blue dashed line represents companions of strongly star-forming hosts, while the red solid line is quiescent hosts. From this plot, we see that strongly star-forming central galaxies tend to have relatively brighter companions than quiescent centrals.

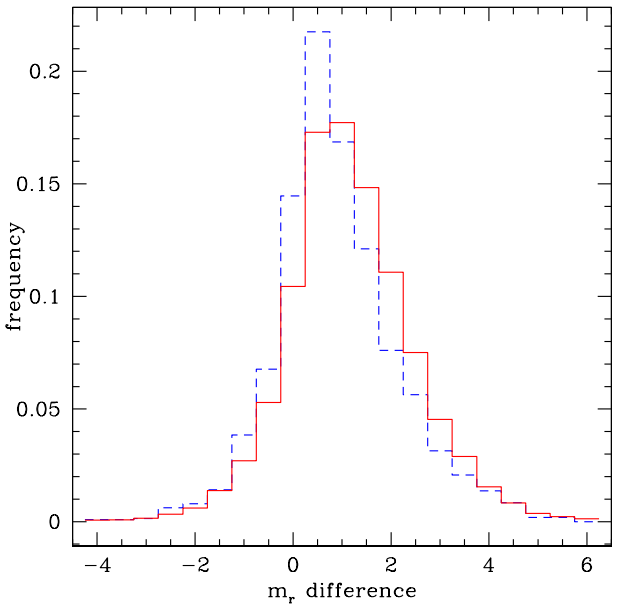

Figure 5. Histogram of the differences in apparent r-band magnitude for each companion and its host. The blue dashed line is for companions of centrals with EW(Hα)$\geq$ 35 Å and the red solid line is companions of centrals with EW(Hα)$<$ 35 Å.

5 DISCUSSION

In summary, we selected a sample of isolated galaxies from the Sloan Digital Sky Survey, and by employing a Monte-Carlo resampling technique, demonstrated that strongly star-forming and quiescent galaxies exhibit different probabilities of having a close companion, even when samples are selected to have matching redshift and stellar mass distributions. When using EW(Hα) as a proxy for star formation, these differences are small (star-formers are $\sim$ 5% more likely to have a close neighbor) but highly significant ($P_{KS} =\sim 10^{-3}$). Thus, we have shown that strongly star-forming and quiescent galaxies exhibit different radial distributions of photometric companions.

We summarize our primary result in Figure 6, which is similar to Figure 4(b), but here we plot the difference in the cumulative fraction of strongly star-forming and quiescent central galaxies as a function of separation. We are again using EW(Hα) = 35 Å as the dividing criterion to separate star-forming and quiescent galaxies. The maximum difference is 5$\pm$ 2% in the 55 kpc radius bin. We explored the effects of using different EW(Hα)cutoffs in our simulations, and the results are described in 3.

There are several possible explanations for the 5% excess in companions seen for the strongly star-forming central galaxies. One possibility is that galaxies are more likely to be star forming if they have a close companion – that is, some small fraction of these star forming galaxies ($\sim$ 5%) are star forming *because* they are experiencing an interaction with a close companion. This is a mechanism that has been well-documented in previous studies (Larson & Tinsley 1978; Barton et al. 2000; Lambas et al. 2003; Woods et al. 2006; Mihos & Hernquist 1994). Alternatively, there is something else about having an elevated star formation rate that increases a galaxy's likelihood to have a close companion. One possibility is that objects that are currently accreting gas via "cold mode" deposition are more likely to have companionship, as this source of fuel is usually associated with larger-scale filamentary over-densities in galaxy positions (see Kereš et al. 2009, and references therein).

Finally, it is possible that there is some systematic error in the determination of M_* which would obscure the fact that the strongly star-forming central galaxies in our sample reside in more massive haloes than the less strongly star-forming central galaxies. However, this is unlikely, be-

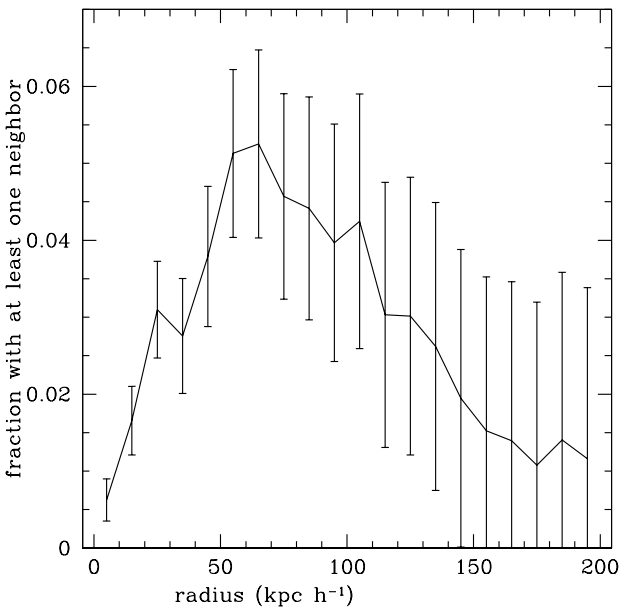

[]

Figure 6. The difference in the cumulative fraction of strongly star-forming and quiescent central galaxies with a neighbor within a given radius. Strongly star-forming central galaxies have EW(Hα)$\geq$ 35 Å.

cause red galaxies (which generally have lower star formation rates) tend to be in higher mass haloes than blue galaxies.

REFERENCES

Adelman-McCarthy J., Ag\\"ueros M., Allam S., Allende Prieto C., Anderson K., Anderson S., Annis J., Bahcall N., Bailer-Jones C., Baldry I., Others 2008, The Astrophysical Journal Supplement Series, 175, 297

Agustsson I., Brainerd T. G., 2007, in Bulletin of the American Astronomical Society Vol. 38 of Bulletin of the American Astronomical Society, Anisotropic Locations of Satellite Galaxies. pp 741–+

Azzaro M., Patiri S. G., Prada F., Zentner A. R., 2007, Monthly Notices of the Royal Astronomical Society, 376, L43

Bailin J., Power C., Norberg P., Zaritsky D., Gibson B. K., 2008, Monthly Notices of the Royal Astronomical Society, 390, 1133

Barnes J. E., Hernquist L., 1996, The Astrophysical Journal, 471, 115

Barton E. J., Geller M. J., Kenyon S. J., 2000, Astrophysical Journal, 530, 660

Blanton M., Hogg D., Bahcall N., Brinkmann J., Britton M., Connolly A., Csabai I., Fukugita M., Loveday J., Meiksin A., Others 2003, The Astrophysical Journal, 592, 819

Blanton M. R., Schlegel D. J., Strauss M. a., Brinkmann J., Finkbeiner D., Fukugita M., Gunn J. E., Hogg D. W., Ivezić v., Knapp G. R., Lupton R. H., Munn J. a., Schneider D. P., Tegmark M., Zehavi I., 2005, The Astronomical Journal, 129, 2562

Chen J., 2008, Astronomy and Astrophysics, 484, 347

Chen J., Kravtsov A. V., Prada F., Sheldon E. S., Klypin A. A., Blanton M. R., Brinkmann J., Thakar A. R., 2006, Astrophysical Journal, 647, 86

Cox T. J., Jonsson P., Primack J. R., Somerville R. S., 2006, Monthly Notices of the Royal Astronomical Society, 373, 1013

Dressler A., 1980, The Astrophysical Journal, 236, 351

Kang X., van den Bosch F. C., Yang X., Mao S., Mo H. J., Li C., Jing Y. P., 2007, Monthly Notices of the Royal Astronomical Society, 378, 1531

Kereš D., Katz N., Fardal M., Davé R., Weinberg D. H., 2009, Monthly Notices of the Royal Astronomical Society, 395, 160

Lambas D., Tissera P., Alonso M., Coldwell G., 2003, Monthly Notices of the Royal Astronomical Society, 346, 1189

Lambas D. G., Tissera P. B., Alonso M. S., Coldwell G., 2003, Monthly Notices of the Royal Astronomical Society, 346, 1189

Larson R. B., Tinsley B. M., 1978, Astrophysical Journal, 219, 46

Masjedi M., Hogg D. W., Blanton M. R., 2008, Astrophysical Journal, 679, 260

Mihos J., Hernquist L., 1994, The Astrophysical Journal, 425, L13

Nikolic B., Cullen H., Alexander P., 2004, Monthly Notices of the Royal Astronomical Society, 355, 874

Postman M., Geller M., 1984, The Astrophysical Journal, 281, 95

Sales L., Lambas D. G., 2005, Monthly Notices of the Royal Astronomical Society, 356, 1045

Tollerud E. J., Bullock J. S., Graves G. J., Wolf J., 2011, The Astrophysical Journal, 726, 108

van den Bosch F. C., Yang X., Mo H. J., Norberg P., 2005, Monthly Notices of the Royal Astronomical Society, 356, 1233

Woods D. F., Geller M. J., Barton E. J., 2006, The Astronomical Journal, 132, 197

Zehavi I., Zheng Z., Weinberg D. H., Blanton M. R., Bahcall N. A., Berlind A. A., Brinkmann J., Frieman J. A., Gunn J. E., Lupton R. H., Nichol R. C., Percival W. J., Schneider D. P., Skibba R. A., Strauss M. A., Tegmark M., York D. G., 2011, Astrophysical Journal, 736, 59

Zentner A. R., Berlind A. a., Bullock J. S., Kravtsov A. V., Wechsler R. H., 2005, The Astrophysical Journal, 624, 505